Synthesis, Characterization, and Micellization Behavior of Poly(L-lactide) and Poly(ethylene glycol) Block Copolymers in the presence of a Novel Organocatalyst

YAN WANG[a], JIN-HUA WANG[a], JUN-HUA BAI[a] AND LI-FANG ZHANG*[,a,b]

[a]*School of Chemistry & Material Science, Shanxi Normal University, Linfen 041004, P.R. China*

[b]*Collaborative Innovation Center for Shanxi Advanced Permanent Magnetic Materials and Technology, Linfen 041004, P.R. China*

ABSTRACT

Biodegradable poly(L-lactide)-poly(ethyleneglycol)-poly(L-lactide) (PLLA-b-PEG-b-PLLA) triblock copolymers and 4-arm star-shaped poly(ethylene glycol)-poly(L-lactide) (4-arm star-shaped PEG-b-PLLA) block copolymers were synthesized via ring-opening polymerization of L-lactide (LLA) in the presence of hydroxyl-terminated α, ω-dihydroxy PEG2000 (PEG2000) and 4-arm PEG as a macroinitiator and 2, 3, 6, 7-tetrahydro-5H-thiazolo [3, 2-a] pyrimidine (ITU) as an organic catalyst. The resultant copolymers were analyzed using various techniques including ^{1}H NMR, FTIR, GPC and DSC. The micellar aggregates were formed from the amphiphilic block copolymers. The relationship between the architecture of block copolymers and their micellization properties, such as critical micelle concentration (CMC) and size of micelles, was investigated. The CMC and micelle size were measured by the steady-state pyrene method and dynamic light scattering, and the results indicated that the formation of micelles became easier for 4-arm star-shaped PEG-b-PLLA copolymer as compared with PLLA-b-PEG-b-PLLA copolymer. The TEM micrographs confirmed the PLLA-core/PEG-shell structure of the micelles.

KEY WORDS : *Poly(L-lactide), Poly(ethylene glycol), Block copolymer, Ring-opening polymerization, Micelles*

INTRODUCTION

Owing to sustainability and eco-friendly properties, bio-based materials have shown remarkable potential to eventually replace petroleum-derived plastics. Poly(L-lactide) (PLLA) derived from renewable resources has attracted wide attention in the field of biomedical applications including biomedical

J. Polym. Mater. Vol. **35,** No. 4, 2018, 393-408

Correspondence author e-mail: zhanglf0015@163.com
DOI : https://doi.org/10.32381/JPM.2018.35.04.1

devices, biodegradable sutures, and bone reparation system due to its biodegradability and biocompatibility[1,2]. PLLA has been reported to possess decent physical properties, such as high strength, thermoplasticity, and fabricability. However, hydrophobicity and poor elasticity have limited the applications of PLLA. As a biocompatible and flexible polymer, PEG presents notable properties such as hydrophilicity, flexibility, nontoxicity, no antigenicity, and immunogenicity in several clinical applications[3]. PEG with the molecular weight of 20000 or less can be metabolized in the human body[4]; hence, its biostability is not an issue. Copolymerization of PEG with lactide is now regarded as a viable means to modulate the hydrophilic/hydrophobic and soft/hard segment ratio and thus, to obtain novel polymeric materials with interesting physical, chemical, and biological properties that are adaptable to specific uses[5-7].

Researchers are increasingly interested in searching for efficient and inexpensive catalysts for the copolymerization of LLA and PEG, and hence, various metal systems have been tested and reported, such as metal oxides (SnO, SnO_2, Sb_2O_3, PbO)[8,9], stannous salts ($SnCl_2$, $SnOct_2$)[10,11], and metal hydrides (NaH and CaH_2)[12,13]. However, these catalysts are more or less cytotoxic. To avoid the metal residues in the final product, more attention has been paid towards the exploration of organic catalysts to replace metal catalysts. In 2001, Nederberg et al.[14] displayed for the first time an organocatalytic approach to the living ROP of lactide using 4-(dimethylamino) pyridine (DMAP). Since then, the strategy of organic catalysis for ROP research has blossomed. A series of widely applied organic catalysts such as *N*-heterocyclic carbenes (NHCs)[15-18], 1, 5, 7-triazabicyclo[4.4.0]dec-5-ene (TBD), 7-methyl-1,5,7-triazabicyclo[4.4.0] dec-5-ene (MTBD), and 1,8-diaza[5.4.0] bicycloundec -7-ene (DBU)[19-23] have also been successfully used as catalysts for ROP of lactide. In 2014, Waymouth and co-workers[24] reported that ITU is capable of the ROP of lactide in the absence of protic initiators to generate cyclic PLA. Moreover, ITU can be prepared from readily available materials via a simple route (Scheme 1). ITU is insensitive to water and oxygen and exhibits outstanding catalytic performance in asymmetric synthesis, which is beneficial for polymerization. Therefore, the ITU-catalyzed ROP is required for synthesis of various polyesters materials.

The amphiphilic block copolymers comprising of PLLA as a hydrophobic segment and PEG as a hydrophilic segment can self-disperse in certain solvents that are good solvents for one block but poor for the other, to form micellar system. Micelles have hydrophilic outer shells and hydrophobic cores in water. Therefore, hydrophobic drugs may be solubilized by the hydrophobic cores of polymeric micelles. These drug loading nanomicelles can escape uptake by the reticuloendothelial system and target tumor locations after intravenous injection[25,26]. In a word, micelle delivery systems can be an efficacious method for disease treatment.

In this research work, a series of PLLA-b-PEG-b-PLLA and 4-arm star-shaped PEG-b-PLLA amphiphilic block copolymers with different molecular weights were synthesized and their

structure, thermal, and crystalline properties were investigated. These polymeric micellization properties such as the CMC, micelle size, and distribution were further analyzed and compared with each other.

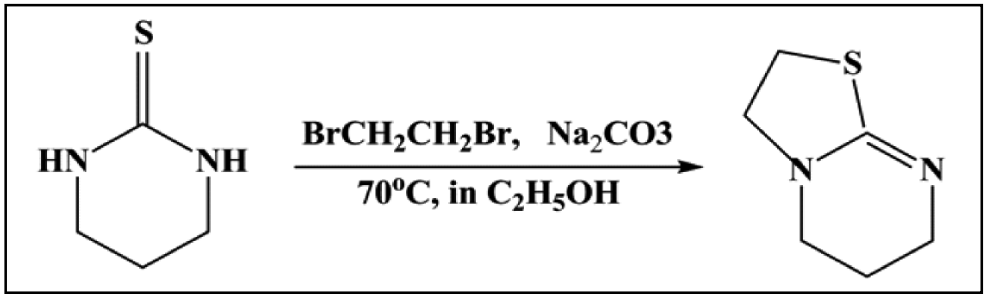

Scheme 1 Synthesis of bicyclic ITU

EXPERIMENTAL

Materials

3,4,5,6-Tetrahydro-2-pyrimidinethiol was purchased from Fluorochem company (UK) and purified by recrystallization twice using absolute ethanol. LLA was synthesized from L-lactic acid and recrystallized three times using dry ethyl acetate and then dried in vacuo at 40°C for 24 h. Dihydroxyl PEG2000 (M_n = 2000 g mol^{-1}) and 4-arm PEG (M_w = 10000 g mol^{-1}) were purchased from Creative PEGWorks company (USA) and dried by an azeotropic distillation with dry toluene. Dichloromethane (CH_2Cl_2) was dried by refluxing over calcium hydride power and distilled prior to use. Toluene was purified before use by refluxing and distillation in the presence of sodium/benzophenone. All the other chemicals employed were of analytical grade and used without further purification.

Catalyst preparation

3,4,5,6-tetrahydro-2-pyrimidinethiol (5.7 g, 50.0 mmol), Na_2CO_3 (6.0 g, 56.6 mmol), absolute ethanol (50.0 mL) and 1,2-dibromoethane (4.5 mL, 50.0 mmol) were added to a round bottom flask under N_2 taking care at 25°C. The reaction mixture was refluxed for 15 h at 70°C, monitored by TLC. The resulting mixture was concentrated under vacuum. The residue was basified using 20% NaOH to pH = 14, extracted three times with CH_2Cl_2, dried over Na_2SO_4, filtered, and concentrated in vacuo to give a pale yellow oil. A crude product was treated with column chromatography (5% MeOH, 5% Et_3N, and 90% CH_2Cl_2) to yield the product (69%) as a clear oil product.

^{1}H NMR (25°C, 600 MHz, $CDCl_3$) spectrum matched the previous reported values[27]: δ 3.56 ppm (t, 2H), 3.40 ppm (t, 2H), 3.27 ppm (t, 2H), 3.15 ppm (t, 2H), 1.88 ppm (m, 2H) (Fig. 1).

Polymerization procedure

All polymerizations were performed in the glass ampoules that were heated, evacuated, and filled with argon for several cycles prior to use. The PLLA-b-PEG-b-PLLA triblock and 4-arm star-shaped PEG-b-PLLA block copolymers were prepared by ROP of LLA using PEG2000 and 4-arm PEG as the initiators and ITU as the catalyst. In a typical procedure, LLA monomer, CH_2Cl_2 solvent, initiator, and catalyst were added to the ampoule successively under a dried argon atmosphere and kept thermostated. The copolymers were precipitated by methanol and dried to a constant mass under vacuum at 40°C.

Characterization of copolymers

NMR spectra were recorded on a Bruker AV-600 MHz spectrometer at room temperature with tetramethylsilane as the internal reference. ^{1}H NMR spectra were referenced using the residual solvent peak at δ 7.27 ppm for deuterated chloroform ($CDCl_3$).

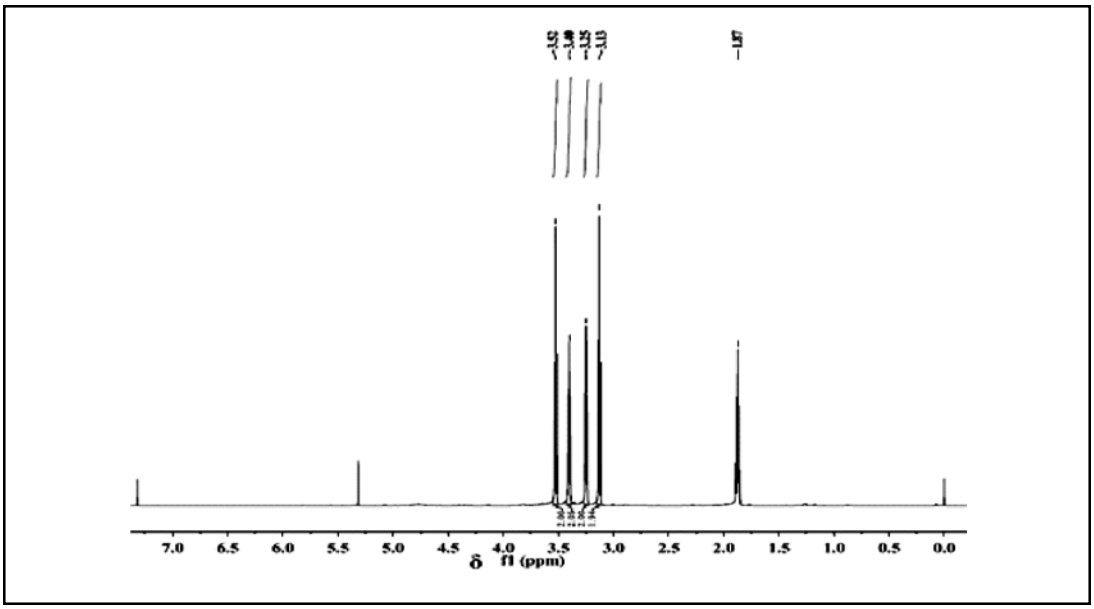

Fig. 1. ^{1}H NMR spectrum of ITU in $CDCl_3$

The molecular weight and polydispersity (PDI) of polymer samples were determined by gel permeation chromatography on the ACQUITY APC instrument equipped with a set of columns (ACQUITY APC XT 200 2.5um, 4.6×150 mm Column and ACQUITY APC XT 451.7 um, 4.6×150 mm Column) and a refractive index detector. Tetrahydrofuran (THF) was used as a mobile phase at the flow rate of 1.0 mL min^{-1} at 25°C. The molecular weights were calibrated using polystyrene standards.

Differential scanning calorimetry (DSC) was carried out on a NETZSCH DSC 200 F3 instrument. Samples were encapsulated into aluminum pans and heated from -60°C to 150°C, held for 2 min to erase their thermal history, and then rapidly cooled down to -60°C. Finally, the samples were heated to 150°C at 10°C min^{-1} under nitrogen flow (70 mL min^{-1}). The melting temperature and glass transition temperature were determined from the endothermal peak.

Fourier transform infrared spectroscopy (FTIR) spectra were recorded with Varian 660 IR spectrometer using KBr pellets.

Micellization

50 mg of the copolymer was dissolved in acetone to produce the total copolymer concentration of 1 mg mL^{-1} and diluted into desired concentration thereafter (ranging from 5×10^{-5} to 1.0 g L^{-1}). Critical micelle concentrations (CMCs) of copolymers were measured by fluorescence spectroscopy method using pyrene as a fluorescence probe[28]. Pyrene concentration was kept at 2×10^{-6} M in acetone. All the fluorescence measurements were performed using CaryEclipse spectrofluorometer. For the emission spectra, detection wavelength was set to 339 nm and the spectral widths of the entrance and exit slits were set at 5 nm. The mean diameter and size distribution of micelles were determined via dynamic light scattering using Nano-ZS90 (Malvern Instrument Ltd). All measurements were made in triplicates and the average particle size and size distribution data were reported at 25°C. The surface morphology of copolymeric microspheres was analyzed using TEM-2100 transmission electron microscopy (TEM). The grid was then left to stand on a piece of filter paper and air dried before measurements.

RESULTS AND DISCUSSION

Synthesis of triblock copolymers

Various PLLA-b-PEG-b-PLLA triblock copolymers were prepared via polymerization of LLA in the presence of PEG2000 and small amounts of ITU. The effects of monomer/initiator molar ratio ([LLA]/[PEG]) and monomer/catalyst molar ratio([LLA]/[C]) on the copolymerization were examined in dried dichloromethane solution at 30°C and the presentative results are shown in Fig. 2 and Table 1, respectively. We observed that within the scope of our study, the optimum [LLA]/[PEG] molar ratio was 200 (Fig. 2). Both the yield and molecular weight of copolymers increased with increasing [LLA]/[PEG] molar ratio from 50 till 200. As the molar ratio increased further ([LLA]/[PEG] > 200), the yield and molecular weight of PLLA-b-PEG-b-PLLA decreased. For the given [LLA]/[PEG] molar ratio of 200, the copolymer molecular weight increased from 2.34×10^4 g mol^{-1} to 2.78×10^4 g mol^{-1} as [LLA]/[C] molar ratio increased from 25 to 30 (Table 1, Nos. 1 and 2). Further increasing [LLA]/[C] from 30 to 40 (Table 1, Nos. 3 and 4) resulted in a decrease in molecular weight from 2.78×10^4 g mol^{-1} to 2.47×10^4 g mol^{-1} because less active species in the reaction medium decreased the rate of polymerization.

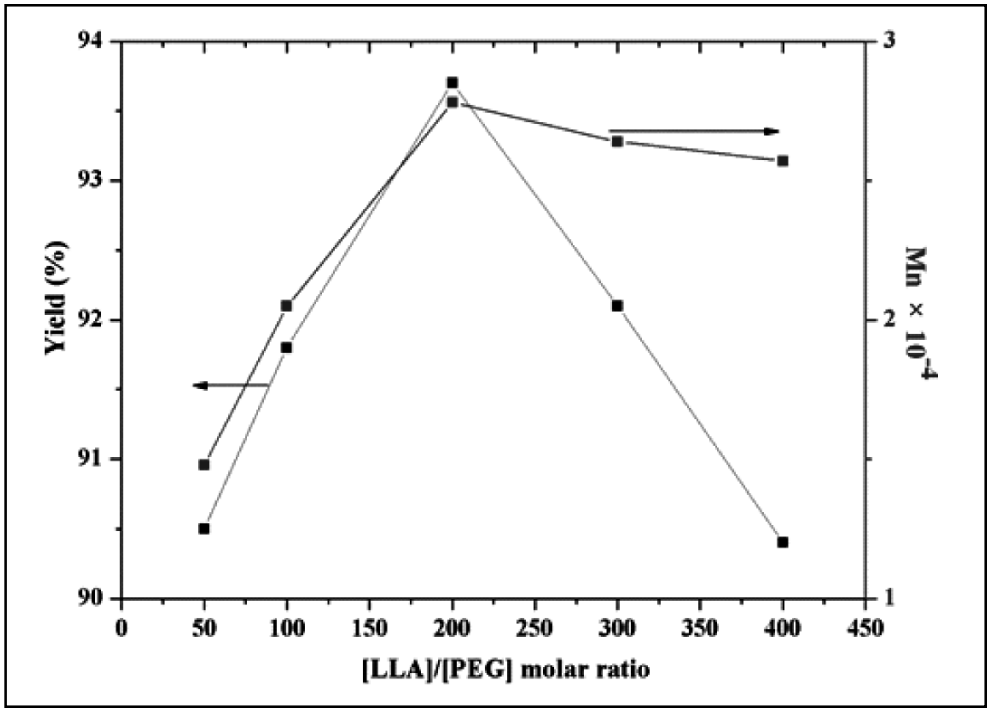

Fig. 2. Effect of the [LLA]/[PEG] molar ratio on the synthesis of PLLA-b-PEG-b-PLLA copolymers Copolymerization conditions: [LLA] = 3.0 mol L^{-1}, [LLA]/[C] = 30, T = 30°C, *t* = 56 h, in CH_2Cl_2

TABLE 1. Effect of the [LLA]/[C] molar ratio on the synthesis of PLLA-b-PEG-b-PLLA copolymers[a]

No.	[LLA]/[PEG] (molar ratio)	[LLA]/[C] (molar ratio)	Yield[b] (%)	M_n[c]×10^{-4} (g mol^{-1})	M_w[c]×10^{-4} (g mol^{-1})	PDI[d]
1	200	25	88.1	2.34	2.93	1.25
2	200	30	94.7	2.78	3.42	1.23
3	200	35	92.4	2.66	3.11	1.17
4	200	40	91.5	2.47	2.87	1.16

[a]Copolymerization conditions: [LLA] = 3.0 mol/L, T = 30°C, *t* = 56 h. [b]Reaction yield. [c]M_n, M_w determined by GPC. [d]PDI determined by GPC.

Table 2 provides the effects of reaction temperature and time on molecular weight and yield of PLLA-b-PEG-b-PLLA copolymer. As shown in Table 2, 30°C was the most suitable temperature for copolymerization. The yield and molecular weight of PLLA-b-PEG-b-PLLA copolymer increased with the elevated temperature in the range of 20-30°C. Higher temperature accelerated intermolecular transesterification and caused broader molecular weight distribution. In addition, polymerization time also significantly affected the synthesis of PLLA-b-PEG-b-PLLA copolymer. We found that the yield and molecular weight increased with increasing of time at 30°C until 56 h, after which, the yield and molecular weight of PLLA-b-PEG-b-PLLA copolymers began to decrease. Thus, the suitable conditions for the copolymerization in CH_2Cl_2 are [LLA]/[PEG] = 200, [LLA]/[C] = 30, 30°C, and 56 h.

TABLE 2. Effects of reaction temperature and time on the synthesis of PLLA-b-PEG-b-PLLA copolymers[a]

No.	T (°C)	*t* (h)	Yield[b] (%)	M_n[c]×10^{-4} (g mol^{-1})	M_w[c]×10^{-4} (g mol^{-1})	PDI[d]
1	30	35	65.3	1.24	1.34	1.08
2	30	45	87.7	1.38	1.56	1.13
3	30	65	88.9	1.35	1.69	1.25
4	30	75	82.6	1.11	1.41	1.27
5	20	56	89.1	0.85	0.98	1.15
6	25	56	93.7	2.44	2.85	1.17
7	30	56	94.7	2.78	3.42	1.23
8	35	56	90.2	1.36	1.82	1.34

[a]Copolymerization conditions: [LLA] = 3.0 mol L^{-1}, [LLA]/[C]= 30, [LLA]/[PEG] = 200, in CH_2Cl_2 as solvent. [b]Reaction yield. [c]M_n, M_w determined by GPC. [d]PDI determined by GPC.

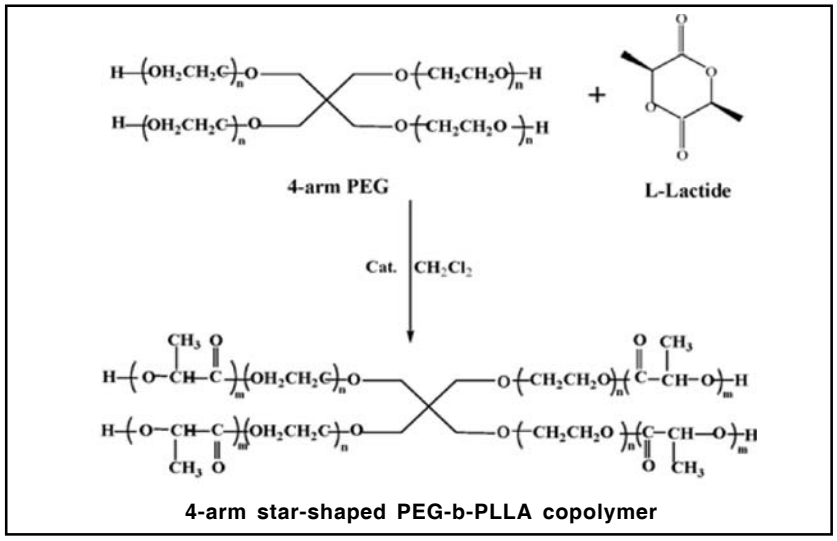

Scheme 2. Synthesis route of 4-arm star-shaped PEG-b-PLLA copolymer

Synthesis of 4-arm star-shaped copolymers

4-Arm star-shaped PEG-b-PLLA copolymers were synthesized in the presence of ITU as the catalyst using 4-arm PEG as the initiator, as shown in Scheme 2. The relationships of reaction temperature and time with copolymerization yield and molecular weight of 4-arm star-shaped PEG-b-PLLA copolymers are summarized in Table 3. The results indicate

TABLE 3. Effects of reaction time and temperature on the synthesis of 4-arm star-shaped PEG-b-PLLA copolymers[a]

No.	T (°C)	*t* (h)	Yield[b] (%)	M_n[c]×10^{-4} (g mol^{-1})	PDI[d]
1	30	32	79.6	5.94	1.01
2	30	36	87.4	6.18	1.02
3	30	39	94.2	6.23	1.04
4	30	42	93.9	6.15	1.08
5	30	45	89.1	6.01	1.12
6	20	39	79.1	5.72	1.02
7	25	39	86.7	6.18	1.23
8	35	39	87.2	5.76	1.14
9	40	39	79.3	5.32	1.27

[a]Copolymerization conditions: [LLA] = 3.0 mol L^{-1}, [LLA]/[C] = 30, [LLA]/[4-arm PEG] = 600, in CH_2Cl_2.
[b]Reaction yield. [c]M_n determined by GPC. [d]PDI determined by GPC.

that 30°C and 39 h were the optimum temperature and time and the copolymer with a yield of 94.2% and molecular weight of 6.15×10^4 g mol^{-1} was obtained. At a higher temperature (> 30°C, Table 3, Nos. 8 and 9), the resultant copolymers were easily degraded, where as below the optimum temperature (< 30°C, Table 3, Nos. 6 and 7) the polymerization reaction proceeded slowly. A prolonged reaction time after monomer consumption often broadened the polydispersity index, possibly due to adverse transesterification side reactions.

Structure Characterization of the copolymers

^{1}H NMR analysis (see Figs. 3A and 3B) shows ^{1}H NMR spectra of PLLA-b-PEG-b-PLLA and 4-arm star-shaped PEG-b-PLLA block copolymers obtained with peak assignments. There were clear, typical signals for both PEG2000 and PLLA blocks. For the PLLA-b-PEG-b-PLLA copolymer, the methine (CH) and methyl (CH_3) protons in PLLA were found at around 5.17 ppm (Fig. 3A, b) and 1.57 ppm (Fig. 3A, a), respectively. Tetralet and double split peaks were observed accordingly, which are in good accordance with the NMR split theory. The methene protons in CH_2 group of PEG2000 were observed around 3.63 ppm (Fig. 3A, c). Besides, for 4-arm star-shaped PEG-b-PLLA copolymer, the α-methylene groups of PLLA-connecting EG units (PLLA-COO-CH_2) appeared at 4.30 ppm (Fig. 3B, a′), while the β-methylene protons (Fig. 3B, b′) remained unchanged at 3.71 ppm. The methylene proton of 4-arm PEG main chain resonated at 3.60 ppm. The above analysis shows that macromonomer PEG and LLA underwent copolymerization while there were few end functional groups which remained unreacted.

The block copolymerizations were further confirmed by GPC approach. All the traces of the linear PLLA-b-PEG-b-PLLA and 4-arm star-shaped block copolymers showed sharp and unimodal distribution as shown in Fig. 4 (curve B and curve D), indicating that the block copolymers were successfully synthesized. In other words, the block copolymers did not contain unreacted PEG2000 or 4-arm PEG and PLLA homopolymer. As we can observe in the GPC curves, the number average molecular weights of linear PLLA-b-PEG-b-PLLA and 4-arm star-shaped block copolymers were much higher than those of the corresponding PEG2000 and 4-arm PEG precursors.

FTIR spectra of the products exhibited absorption bands related to both PEG/4-arm PEG and PLLA blocks (Fig. 5). The region of 3500 cm^{-1} showed a broad absorption, which is a characteristic of the hydroxyl groups. The clear and sharp absorption peaks at ~1730 cm^{-1} indicated the presence of the ester carbonyl stretching vibrations. The C-H stretching band of the PEG2000 block centered at 2883~2887 cm^{-1} remained in Fig. 5. The bands at 935 and 650 cm^{-1} are known to be characteristics of LLA monomer, while no absorption peaks were found in the two copolymers. Besides, for 4-arm star-shaped PEG-b-PLLA copolymer, the peaks at 1111.3 cm^{-1} and 1180.9 and 1224.3 cm^{-1} were assigned to the stretching peaks of C-O-C and C(O)-O-C, respectively. All these discussed results suggest that the PLLA-b-PEG-b-PLLA and 4-arm star-shaped copolymers were synthesized successfully.

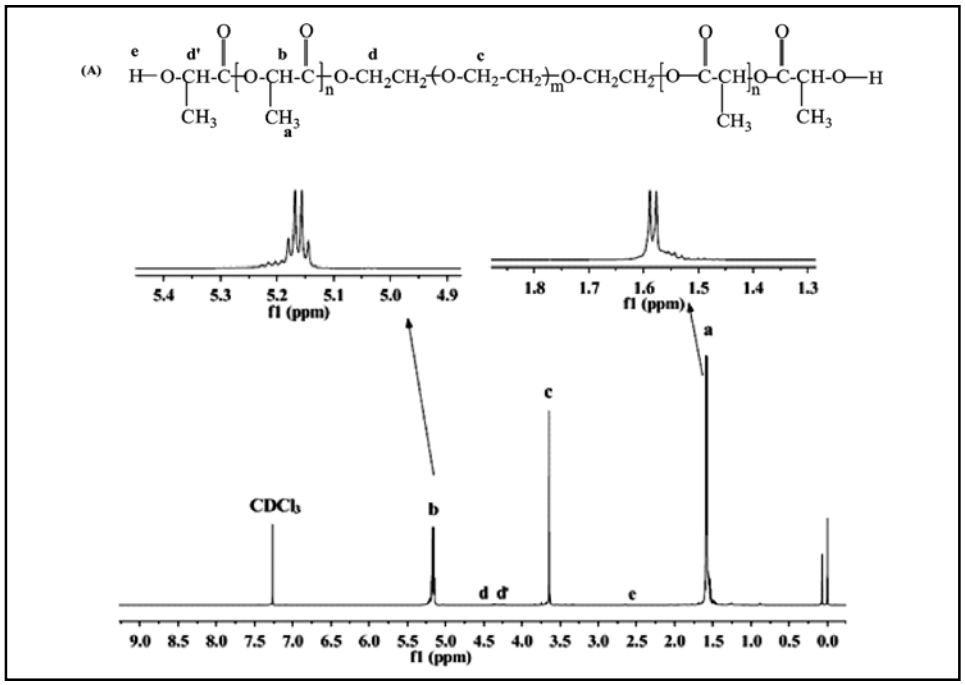

Fig. 3A. ^{1}H NMR spectrum ($CDCl_3$) of typical PLLA-b-PEG-b-PLLA copolymer

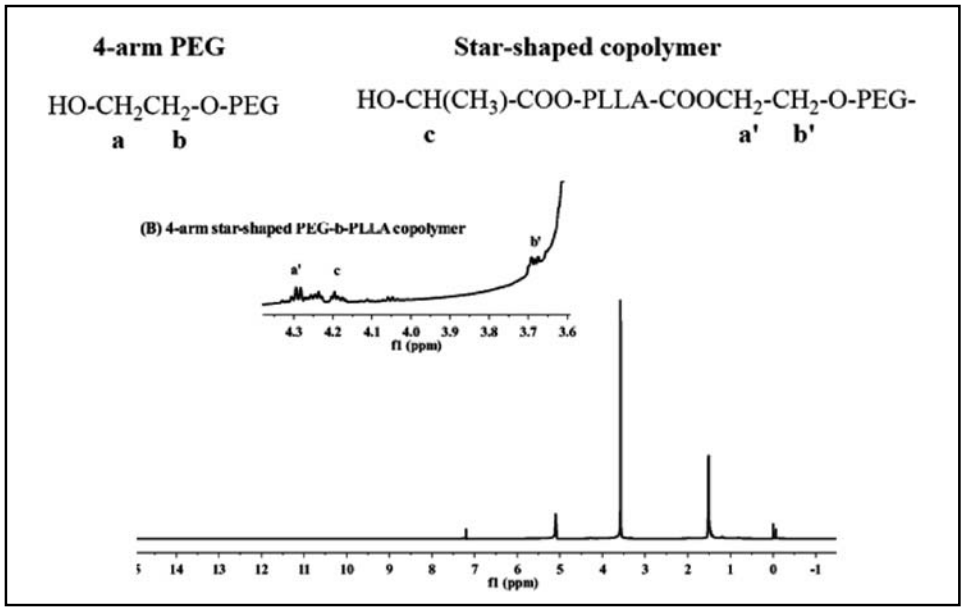

Fig. 3B. ^{1}H NMR spectrum ($CDCl_3$) of a typical 4-arm star-shaped PEG-b-PLLA copolymer

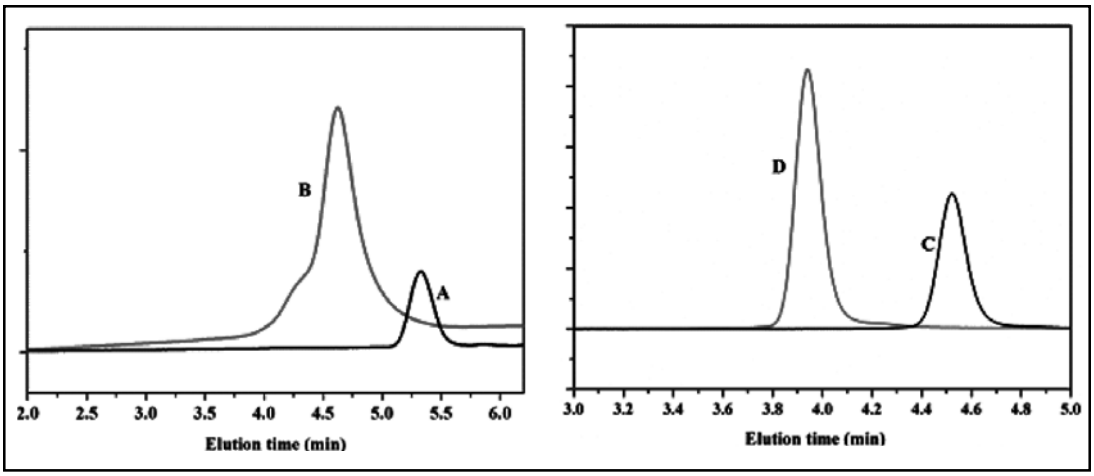

Fig. 4. GPC curves of polymers: PEG2000 (A), linear PLLA-b-PEG-b-PLLA copolymer (B), 4-arm PEG (C), and 4-arm star-shaped PEG-b-PLLA copolymer (D)

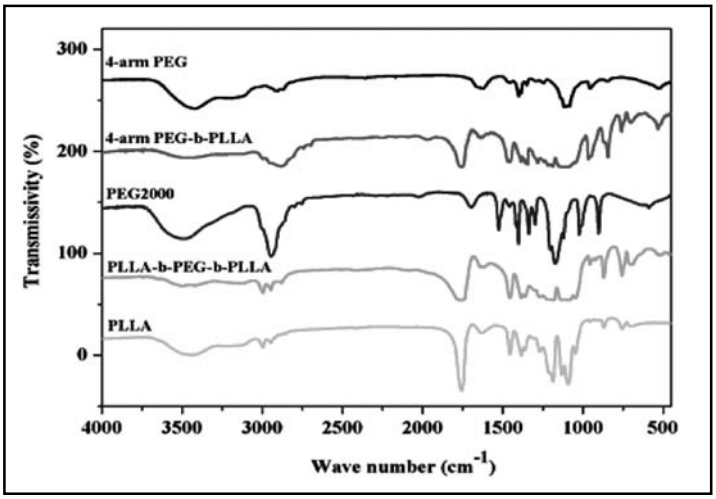

Fig. 5. FTIR spectra of linear PEG-b-PEG-b-PLLA copolymer and 4-arm star-shaped PEG-b-PLLA copolymer

Thermal analysis

The thermal characteristics of PLLA-b-PEG-b-PLLA and 4-arm PEG-b-PLLA copolymers with different molecular weights were investigated using DSC and PEG2000 and PLLA homopolymers were also utilized for comparison. The thermograms of the PEG2000, PLLA, and PLLA-b-PEG-b-PLLA polymers are presented in Fig. 6. PEG2000 (Fig. 6, curve 1) exhibited a usual endothermal melting transition at 52°C[29]. For PLLA-b-PEG-b-PLLA copolymer with a M_n of 3.6×10^3 g mol^{-1} (Fig. 6, curve 2), the melting peak (T_m) shifted from 52°C to 41.9°C for the corresponding

PEG2000 at the second heating. The reduced melting point can be attributed to the presence of short PLLA sequences attached to PEG blocks, probably disrupting the orderly fold pattern of the crystal. As for the copolymer with M_n of 1.97×10^4 g mol^{-1} (Fig. 6, curve 3), an endothermal peak was detected at 167°C, which is in accordance with the melting characteristics of PLLA. However, this endotherm peak of PLLA blocks is lower than the melting point of PLLA at around 173°C (Fig. 6, curve 4). These results indicate that the crystallization of PLLA blocks was disturbed by the existence of PEG blocks. The glass transition (T_g) and crystallization peak (T_c) values were also estimated. As expected, copolymer with M_n of 1.97×10^4 g mol^{-1} showed a clear T_g at 41.7°C and a T_c at 76.1°C (Fig. 6, curve 3), suggesting the miscibility of PLLA and PEG sequences. On the contrary, neither T_g nor T_c was observed for PLLA-b-PEG-b-PLLA copolymer with M_n of 3.6×10^3 g mol^{-1} which crystallized too fast to be made amorphous even by extremely rapid cooling. DSC thermograms revealed that one of melting endotherms in PLLA-b-PEG-b-PLLA triblock copolymers did not appear when the PLLA block length was relatively short and the content was relatively low, which is consistent with the results in the literature[30].

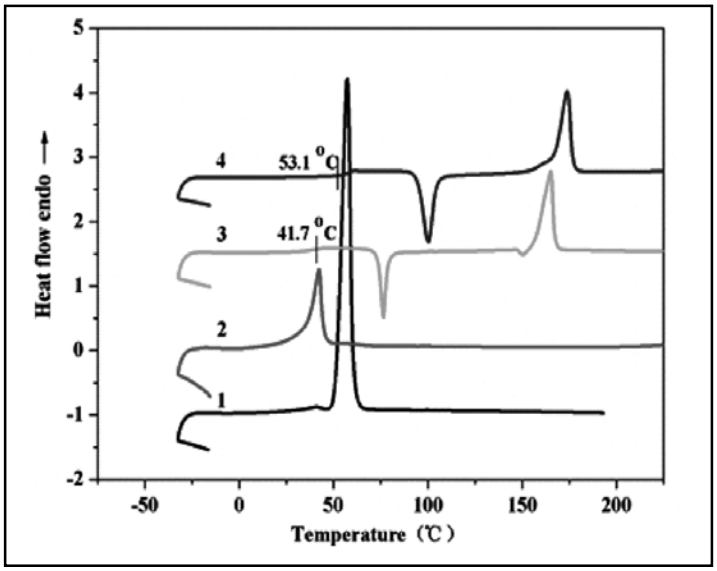

Fig. 6. DSC curves of (1) PEG2000; (2) M_n = 3.6×10^3 g mol^{-1} PLLA-b-PEG-b-PLLA copolymer; (3) M_n = 1.97×10^4 g mol^{-1} PLLA-b-PEG-b-PLLA copolymer; (4) PLLA (at the second heating)

Fig. 7 illustrates the second DSC heating curves of 4-arm PEG, PLLA, and 4-arm star-shaped PEG-b-PLLA copolymers. T_m value of 4-arm PEG (Fig. 7, curve a) was estimated to be 57.7°C, whereas those for star-shaped block copolymers namely curve b and curve c, were estimated as 41.9°C and 35.3°C, respectively. The observed T_m values were related to the

crystallization of 4-arm PEG segments for star-shaped block copolymers. In case of the copolymer with M_n of 6.23×10^4 g mol^{-1} (Fig. 7, curve d), a clear crystallization exothermal peak, T_c, was recorded at 92°C followed by a small melting peak, T_m, at 146.9°C corresponding to PLLA blocks. However, the 4-arm PEG melting endotherm was not detected, indicating that 4-arm PEG segments were phase-mixed with the PLLA (Fig. 7, curve e). Hence, longer is the PLLA chain length, easier it is to crystallize. A similar phenomenon was also found in the linear PLLA-b-PEG-PLLA block copolymers with higher PLLA blocks. Notably, the T_g values of all the copolymers were not clearly observed in the DSC thermograms due to an overlapping with the T_g of PLLA (40-60°C). We can use the above results to conclude that 4-arm PEG blocks and PLLA blocks can both crystallize in different domains when their lengths are long enough, as also reported in the literature[31].

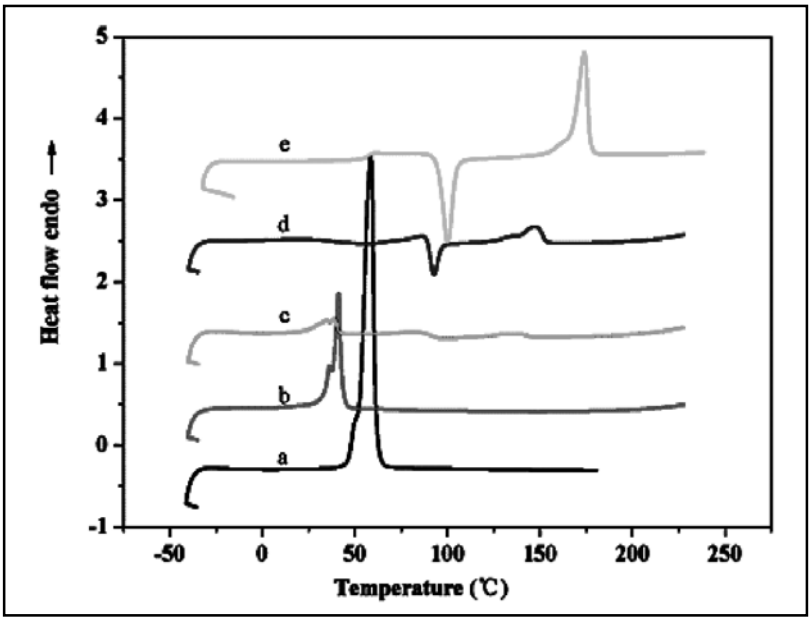

Fig. 7 DSC thermograms of (a) 4-arm PEG; (b)M_n = 2.35×10^4 g mol^{-1} 4-arm star-shaped PEG-b-PLLA copolymer; (c)M_n = 3.72×10^4 g mol^{-1} 4-arm star-shaped PEG-b-PLLA copolymer; (d) M_n = 6.23×10^4 g mol^{-1} 4-arm star-shaped PEG-b-PLLA copolymer; and (e) PLLA

Micellization behavior

The amphiphilic block copolymers can self-assemble to form micelles in a water environment when the block copolymer concentration is higher than the critical micelle concentration (CMC) which characterizes the micelle stability[32]. CMCs were determined using fluorescence spectroscopy using pyrene as a hydrophobic probe. Fig. 8 shows the emission spectra of pyrene as the function of the copolymer concentration in water solution. As the concentration of copolymer was

increased, a red-shift of pyrene was observed in the emission spectrum. This red-shift resulted from pyrene moving into the micelle cores (hydrophobic) from the aqueous phase, which resulted in an alteration in the intensity (I_{383}/I_{372}) of pyrene fluorescence band. Plots of the intensity ratio I_{383}/I_{372} from the emission spectra versus copolymer concentration are displayed in Fig. 9. At low concentrations of the copolymer, I_{383}/I_{372} band fluorescence intensity ratio was essentially constant. As the concentrations of the copolymer increased, the band intensity ratio started to increase significantly at a certain copolymer concentration where the CMC value was determined from the intersection point of two straight lines. CMCs were 1.73×10^{-3} g L^{-1} and 5.68×10^{-4} g L^{-1}, respectively, for linear PLLA-b-PEG-b-PLLA and 4-arm star-shaped PEG-b-PLLA, as shown in Fig. 9. Notably, CMC value of 4-arm star-shaped copolymer was lower than the linear copolymer, indicating that the micelle formation became easier as the number of arms in the block system increased. This could be because the covalent bond character of a star-shaped block copolymer facilitates micellization as the unimer state of a star-shaped block copolymer with several arms resembles the micellar state.

The hydrodynamic diameter of particles was measured by dynamic light scattering (DLS).

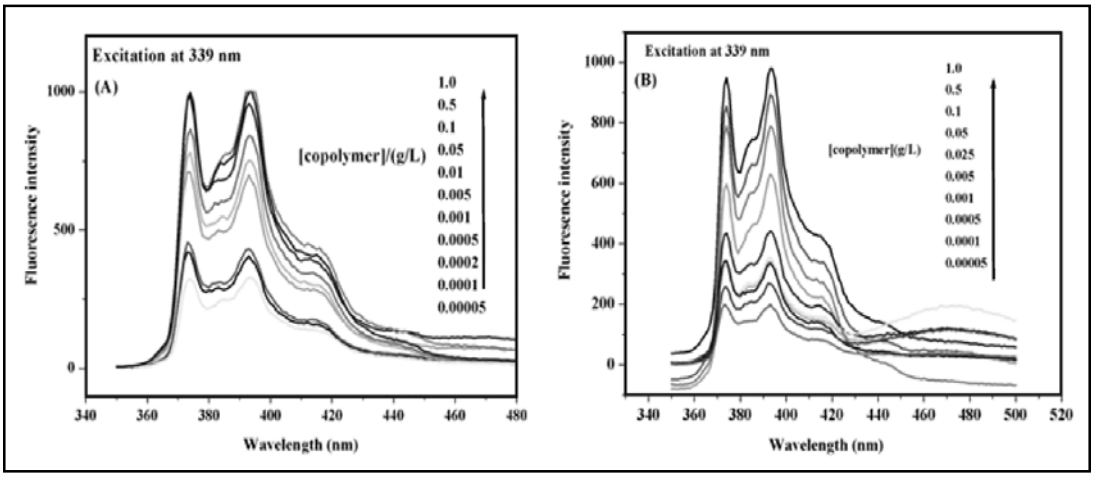

Fig. 8. Emission spectra of pyrene as a function of copolymer concentration
(A) linear PLLA-b-PEG-b-PLLA copolymer; (B) 4-arm star-shaped PEG-b-PLLA copolymer.

Fig. 10 presented the size distribution of triblock and 4-arm star-shaped copolymer micelles. The average diameters of micelles were 98.1 nm and 120.6 nm for triblock and star-shaped copolymers, respectively. It was interest to note that the arm star-shaped copolymer exhibited higher micelle sizes than the linear copolymer, which could be assigned to the longer PLLA block length.

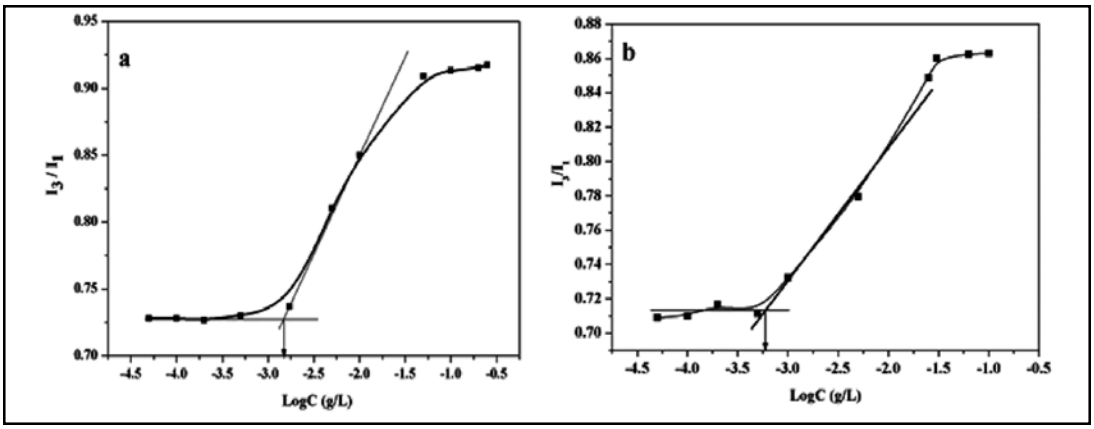

Fig. 9 Determination of the CMC of copolymers: (a) linear PLLA-b-PEG-b-PLLA copolymer, and (b) 4-arm star-shaped PEG-b-PLLA copolymer. The concentration at the intersection of two straight lines corresponds to the CMC

The nanoparticles of linear and star-shaped copolymers were observed with TEM. The micrographs are typical of those obtained for all the samples, confirming that both the types of copolymers formed spherical, discrete particles in an aqueous media (Fig. 11). The polymeric micelles formed from the PLLA-b-PEG-b-PLLA and 4-arm star-shaped PEG-b-PLLA copolymers may be used to encapsulate the hydrophobic drugs and to deliver them via parenteral administrations. Further studies are underway to evaluate the potential of these systems for controlled delivery of drugs in our laboratory.

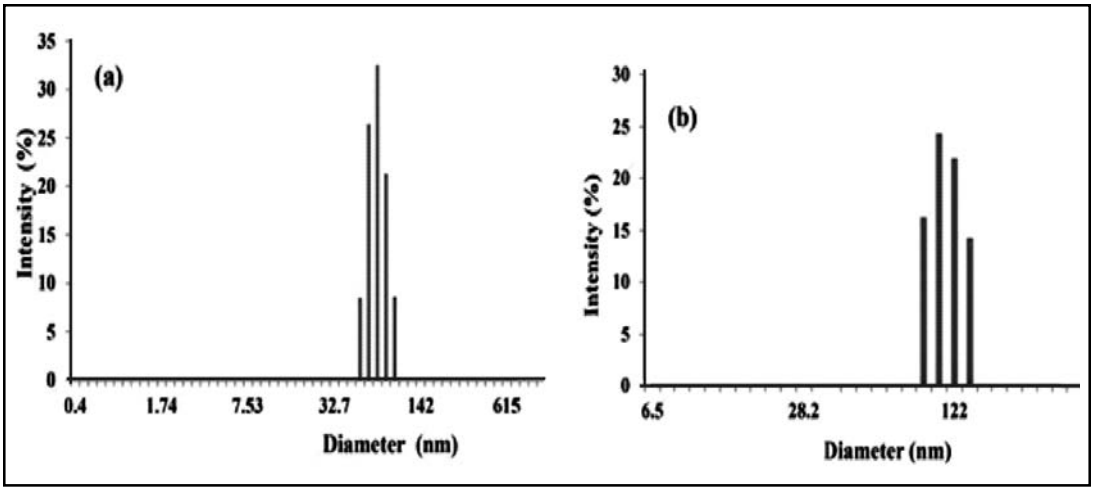

Fig. 10 The micelle size distribution of copolymers: (a) linear PLLA-b-PEG-b-PLLA copolymer, and (b) 4-arm star-shaped PEG-b-PLLA copolymer

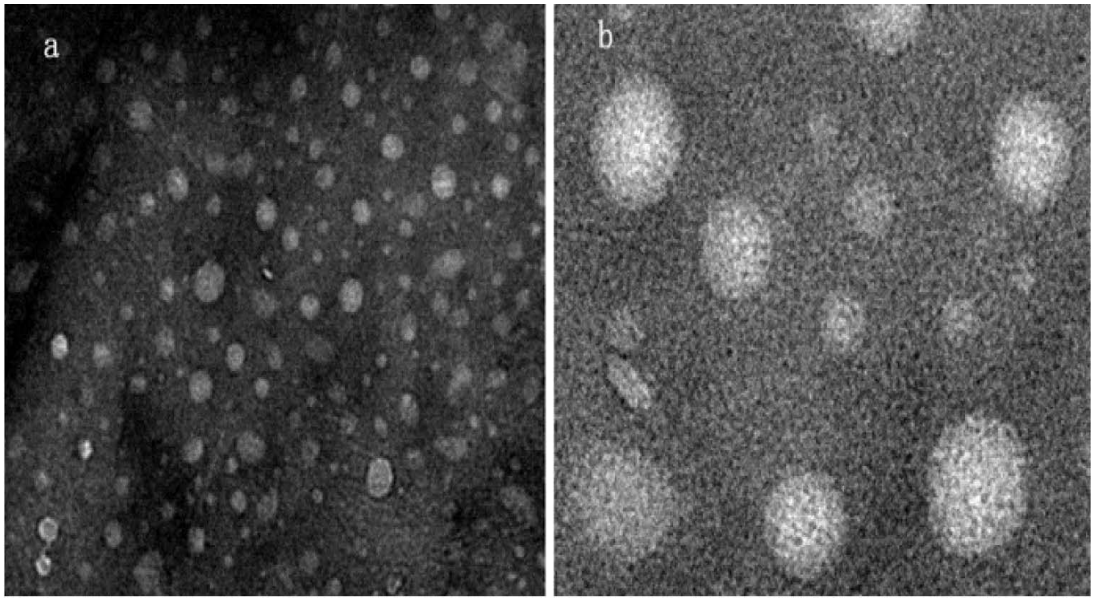

Fig. 11. TEM graphs of linear PLLA-b-PEG-b-PLLA copolymer (a) and 4-arm star-shaped PEG-b-PLLA copolymer (b) micelle-like nanoparticles

CONCLUSIONS

In this work, we have shown that 2, 3, 6, 7-tetrahydro-5H-thiazolo [3, 2-a] pyrimidine is an effective catalyst for the preparation of linear PLLA-b-PEG-b-PLLA and 4-arm star-shaped PEG-b-PLLA copolymers with different molecular weights. These block copolymers were characterized by GPC, NMR, DSC techniques. These amphipathic block copolymers could easily form nano-micelles in an aqueous solution using the solvent-dialysis method. The size of micelles and CMC were measured by the pyrene fluorescene method and DLS analysis.

Acknowledgement

This work was supported by Basic Research Project of Shanxi Province of China (No.2015011029) and Shanxi Province Education Innovation Project for Postgraduated (No.2015BY38).

REFERENCES

1. D. D. Zhou, J. Shao, G. Li, J. R. Sun, X. C. Bian and S. X. Chen. *Polymer* **62** (2015) 70.
2. S. Nagarajan, K. Deepthi and E. B. Gowd. *Polymer* **105** (2016) 422.
3. S. M. Li, X. H. Chen, R. A. Gross and S. P. McCarthy. *J. Mater. Sci. Mater. Med.* **11** (2000) 227.
4. T. B. T. Nguyen, S. M. Li and A. Deratani. *Int. J. Pharm.* **495** (2015) 154.
5. Y. Bakkour, V. Darcos, F. Coumes, S. M. Li and J. Coudare. *Polymer* **54** (2013) 1746.
6. T. Watanabea, Y. Sakamotoa, T. Inookab and Y. Kimurab. *Colloids and surfaces A: physicochem. Eng. Aspects* **520** (2017) 764.

7. V. Shalgunov, D. Zaytseva-Zotova, A. Zintchenko, T. Levada, Y. Shilov, D. Andreyev, D. Dzhumashev, E. Metelkin, A. Urusova, O. Demin, K. McDonnell, G.Troiano, S. Zale and E. Safarovà. *J. Controlled Release* **261** (2017) 31.

8. H. R. Kricheldorf and J. Meier-Haack. *Makromol. Chem.* **194** (1993) 715.

9. X. M. Deng, C. D. Xiong, L. M. Cheng and R. P. Xu. *J. Polym. Sci., Part C: Polym. Lett.* **28** (1990) 411.

10. H. R. Kricheldorf and C. Boettcher. *Makromol. Chem., Makromol. Symp.***73** (1993) 47.

11. P. Jie, S. S. Venkatraman, M. Feng, B. Y. C. Freddy and G. L. Huat. *J. Controlled Release* **110** (2005) 20.

12. Z. Jedlinski, P. Kurcok, W. Walach, H. Janeczek and I. Radecka. *Makromol. Chem.* **194** (1993) 1681.

13. I. Rashkov, N. Manolova, S. M. Li, J. L. Espartero and M. Vert. *Macromolecules* **29** (1996) 50.

14. F. Nederberg, E. F. Connor, M. Moller, T. Glauser and J. L. Hedrick. *Angew. Chem., Int. Ed.* **40** (2001) 2712.

15. J. H. Bai, N. Wu, Y. Wang, Q. R. Li, X. Q. Wang and L. F. Zhang. *RSC Adv.* **6** (2016) 108045.

16. L. Guo and D. H. Zhang. *J. Am. Chem. Soc.* **131** (2009) 18072.

17. L. Guo, S. H. Lahasky, K. Ghale and D. H. Zhang. *J. Am. Chem. Soc.* **134** (2012) 9163.

18. M. Fèvre, J. Pinaud, Y. Gnanou, J. Vignolle and D. Taton. *Chem. Soc. Rev.* **42** (2013) 2142.

19. A. P. Dove. *ACS Macro. Lett.* **1** (2012) 1409.

20. A. Chuma, H. W. Horn, W. C. Swope, R. C. Pratt, L. Zhang, B. G. G. Lohmeijer, C. G. Wade, R. M. Waymouth, J. L. Hedrick and J. E. Rice. *J. Am. Chem. Soc.* **130** (2008) 6749.

21. P. Olsén, T. Borke, K. Odelius and A. C. Albertsson. *Biomacromolecules* **14** (2013) 2883.

22. X. Wang, S. D. Cui, Z. J. Li, S. L. Kan, Q. G. Zhang, C. X. Zhao, H. Wu, J. J. Liu, W. Z. Wu and K. Guo. *Polym. Chem.* **5** (2014) 6051.

23. R. Todd, S. Tempelaar, G. L. Re, S. Spinella, S. A. McCallum, R. A. Gross, J. M. Raquez and P. Dubois. *ACS Macro Lett.* **4** (2015) 408.

24. X. Y. Zhang and R. M. Waymouth. *ACS Macro. Lett.* **3** (2014) 1024.

25. A. K. Singla, A. Garg and D. Aggarwal. *Int. J. Pharm.* **235** (2002) 179.

26. T. Nakanish, S. Fukushima, M. Suzuki and Y. Matsumura, M. Yokoyama, T. Okano, Y. Sakurai, K. Kataoka and K. Okamoto. *J. Controlled Release* **74** (2001) 295.

27. V. B. Birman, X. M. Li and Z. F. Han. *J. Org. Lett.* **9** (2007) 37.

28. A. Dominguez, A. Fernandez, N. Gonzale, E. Iglesias and L. Montenegro. *J. Chem. Educ.* **74** (1997) 1227.

29. I. Rashkov, N. Manolova, S. M. Li, J. L. Espartero and M. Vert. *Macromolecules* **29** (1996) 50.

30. S. S. Venkatraman, J. Pan, M. Feng, B. Y. C. Freddy and G. Leong-Huat. *Int. J. Pharm.* **298** (2005) 219.

31. P. Carrai, M. Tricoli, L. Lelli, G. D. Guerra, R. Sbarbati Del Guerra, M. G. Cascone and P. Giusti. *J. Mater. Sci.: Mater. Med.* **5** (1994) 308.

32. S. C. Lee, Y. Chang, J. S. Yoon, C. Kim, I. C. Kwon, Y. H. Kim and S. Y. Jeong. *Macromolecules* **32** (1999) 1847.

Received: 12-12-2018

Accepted: 26-01-2019